

JCSDA Infrared Sea Surface Emissivity Model

Paul van Delst

*Joint Center for Satellite Data Assimilation
Cooperative Institute for Meteorological Satellite Studies
Camp Springs MD, USA*

Introduction

The Global Data Assimilation System (GDAS) at NCEP/EMC previously used an infrared sea surface emissivity (IRSSE) model based on Masuda *et al* (1988). This Masuda model doesn't account for the effect of enhanced emission due to reflection from the sea surface (only an issue for larger view angles) and emissivity data was only available at a coarse spectral resolution making application to high resolution instruments, such as AIRS, problematic. The model has been updated to use sea surface emissivities derived via the Wu and Smith (1997) methodology as described in van Delst and Wu (2000). The emissivity spectra are computed assuming the infrared sensors are not polarized and using the data of Hale and Querry (1973) for the refractive index of water, Segelstein (1981) for the extinction coefficient, and Friedman (1969) for the salinity/chlorinity corrections. Instrument spectral response functions (SRFs) are used to reduce the emissivity spectra to instrument resolution. These are the values predicted by the IRSSE model.

The IRSSE Model

A starting point was the sea surface infrared emissivity model, SSIREM, described in Sherlock (1999),

$$\varepsilon(\theta) = c_0 + c_1 \hat{\theta}^{N_1} + c_2 \hat{\theta}^{N_2} \quad (1)$$

where $\hat{\theta} = \frac{\theta}{60^\circ}$ is the normalized view angle, and N_1 and N_2 are integers.

The coefficients c_0 , c_1 , and c_2 for a set of N_1 and N_2 are determined by regression with a maximum residual cutoff of $\Delta\varepsilon = 0.0002$ only for wind speeds of 0ms^{-1} .

In generating the sensor emissivities, it was noticed that the emissivity variation with wind speed was much larger than the 0.0002 residual tolerance used in SSIREM. This is shown in figure 1 where the wind speed variation of computed emissivity with respect to 0.0ms^{-1} for NOAA-17 HIRS channel 8 for view angles $0-65^\circ$ can be much larger than 0.0002 (note that the HIRS only scans out to 50° – the data at large angles is used for fitting purposes only).

Since the sensor emissivity variation with wind speed was greater than 0.0002, the exponents N_1 and N_2 of the emissivity model were also allowed to vary in the fitting process. For integral values of N_1 and N_2 their variation with wind speed suggested inverse relationships for both (see fig.2). When the exponents were changed to floating point values and the fitting exercise repeated, the result showed a smoother relationship (see fig.3).

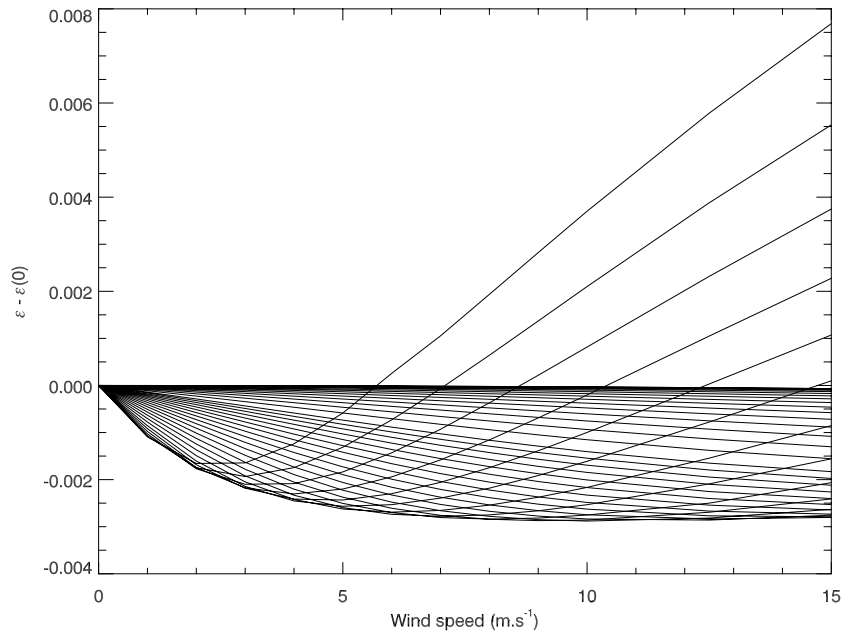


Fig. 1: Wind speed dependence of emissivity for NOAA-17 HIRS channel 8 at view angles 0-65°. (Larger angles used to bound regression fits.)

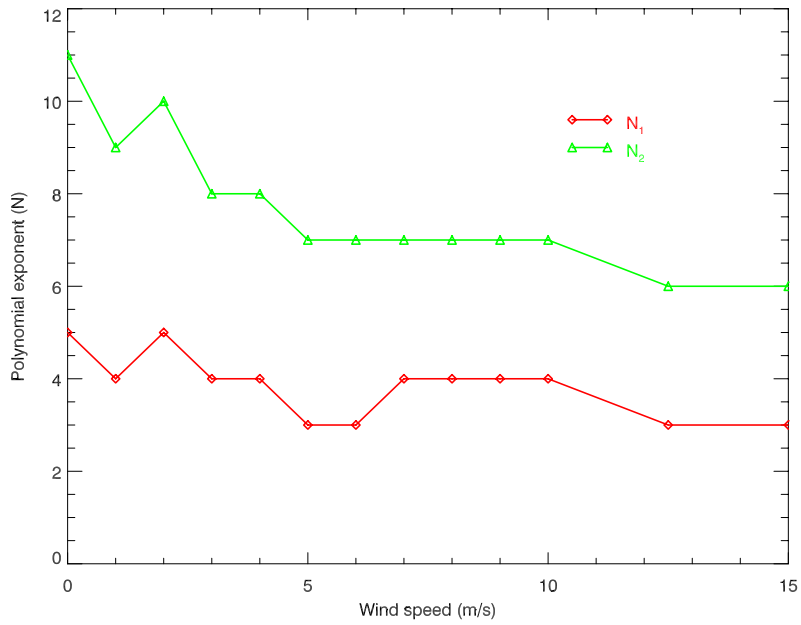


Fig.2: Variation of emissivity fit integral polynomial exponents with wind speed for NOAA-17 HIRS channel 8.

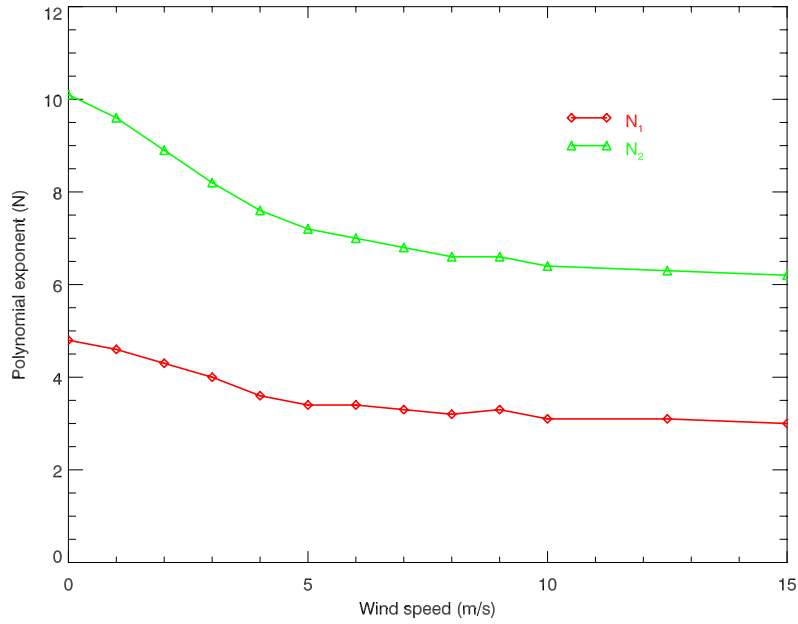


Fig.3: Variation of emissivity fit floating point polynomial exponents with wind speed for NOAA-17 HIRS channel 8.

Based on the smooth variation of the exponents with wind speed shown in figure 3, the emissivity model was changed to,

$$\varepsilon(\theta, \nu) = c_0(\nu) + c_1(\nu)\hat{\theta}^{c_2(\nu)} + c_3(\nu)\hat{\theta}^{c_4(\nu)} \quad (2)$$

where ν is the wind speed in ms^{-1} . In generating the model coefficients, for a series of wind speeds $0\text{-}15\text{ms}^{-1}$, the coefficients c_i were obtained using Levenberg-Marquardt least-squares minimization. Interpolating coefficients for each c_i as a function of wind speed were then determined. In using the model, the c_i are computed for a given wind speed and these computed coefficients are used in equation 2 to calculate the view angle dependent emissivity.

Emissivity Fit Statistics

The emissivity fit RMS residuals for an independent data set are shown for all wind speeds in figure 4 for NOAA-17 HIRS and the Aqua AIRS 281 channel subset. For both instruments, the maximum emissivity fit error was at the 0.00002 level. For instruments that scan out to higher view angles, e.g. GOES instruments, the maximum errors were around 0.0001 at 65° .

To determine the impact of emissivity fit errors on the top-of-atmosphere (TOA) brightness temperatures (T_B), the fitted emissivities were used in radiative transfer calculations. Two tests were run; one determining the impact of emissivity fit errors on the TOA T_B values for all wind speeds, and another to determine the impact when emissivities at only 0.0ms^{-1} are predicted.

The TOA T_B RMS residuals for HIRS and AIRS for all wind speeds are shown in figure 5. The maximum residuals for either instrument never exceeded 0.001K. Figure 6 shows the same RMS residuals, but only for prediction of emissivities at zero wind speed. This shows the expected error if one neglects the wind speed effect on emissivity. The increase in the RMS residuals is about two orders of magnitude which, while a large increase, still results in very small temperatures errors. The maximum errors are about the same magnitudes.

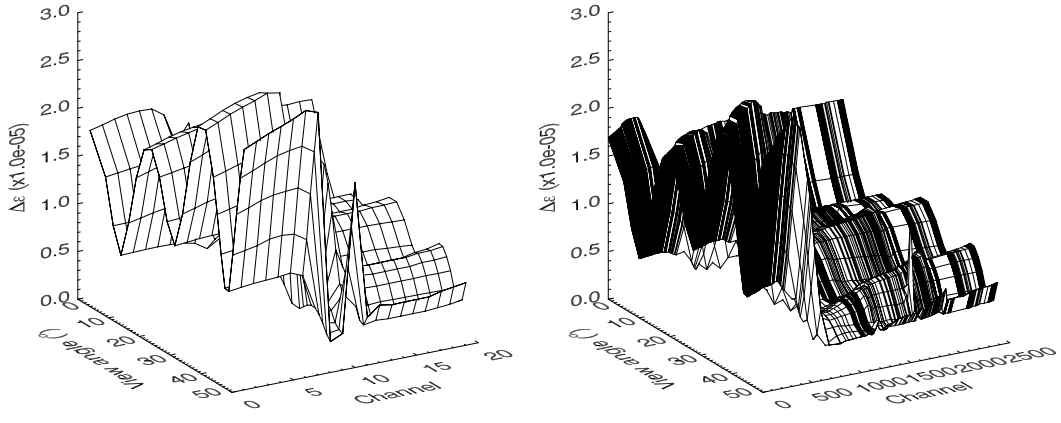


Fig.4: RMS emissivity fit residuals for NOAA-17 HIRS (*left*) and Aqua AIRS 281 channel subset (*right*), all wind speeds 0-15ms⁻¹.

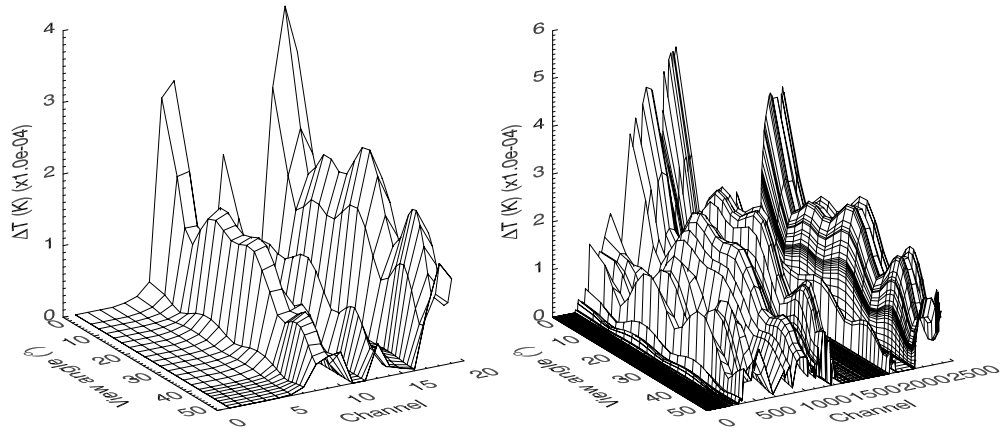


Fig.5: RMS top-of-atmosphere brightness temperature residuals due to emissivity fit for NOAA-17 HIRS (*left*) and Aqua AIRS 281 channel subset (*right*), all wind speeds 0-15ms⁻¹.

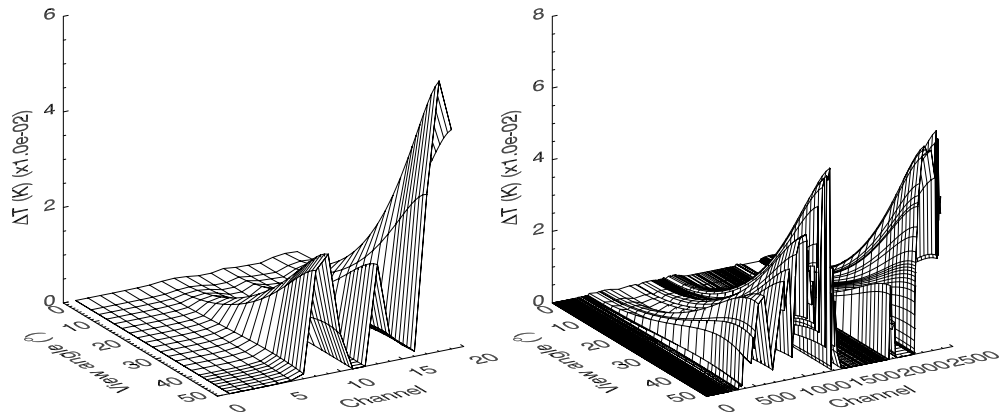


Fig.6: RMS top-of-atmosphere brightness temperature residuals due to emissivity fit for NOAA-17 HIRS (*left*) and Aqua AIRS 281 channel subset (*right*), all wind speeds, but only predicting 0.0ms⁻¹ wind speed emissivities.

The wind speed effect is not as negligible for instruments that scan at larger view angles. The RMS and maximum TOA T_B residuals for the GOES-12 sounder, predicting only zero wind speed emissivities, are shown in figure 7. The residuals are much larger for higher view angles,

becoming significant in terms of instrument noise and general atmospheric transmittance modeling errors.

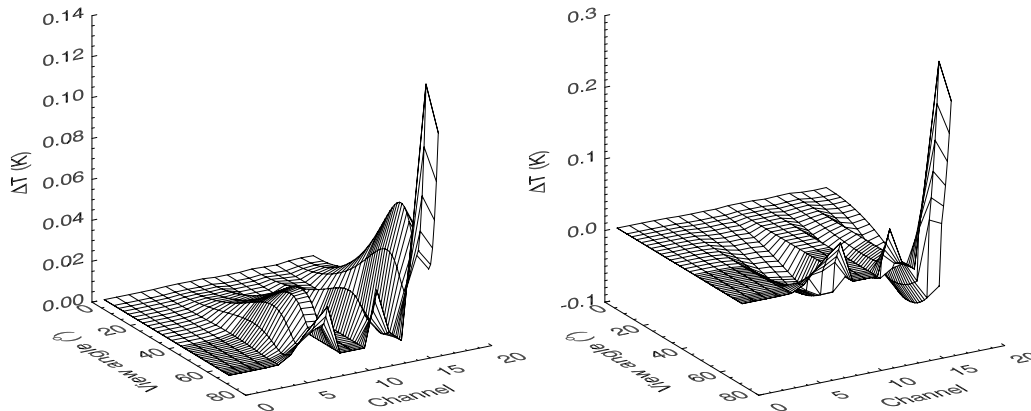


Fig.7: RMS (left) and maximum (right) top-of-atmosphere brightness temperature residuals due to emissivity fit for GOES-12 Sounder, all wind speeds, but only predicting 0.0ms^{-1} wind speed emissivities. Note the larger errors at higher view angle compared to the HIRS and AIRS.

Conclusions

When wind speed is taken into account, the fit residuals are relatively independent of view angle and channel with magnitudes (average, RMS, and maximum) of around $10^{-4} - 10^{-3}\text{K}$. For those instruments with maximum scan angles $<50\text{-}55^\circ$ (e.g. HIRS, AIRS), ignoring the wind speed effect does increase the errors, but to much less than the instrument noise in most cases. When large view angles are used, however, the wind speed dependence of the emissivity must be included to avoid large errors in the result. Given the relative simplicity of the model (see eqn.(2)) and how it was implemented, there is no speed of execution impact in including the wind speed as a predictor.

Acknowledgements

This work was funded under NOAA grant NA07EC0676

References

- Friedman, D. 1969. Infrared characteristics of ocean water. *Appl. Opt.*, **8**, 2073-2078
- Hale, G.M. and Querry, M.R. 1973. Optical constants of water in the 200nm to 200 μm wavelength region. *Appl. Opt.*, **12**, 555-563
- Masuda, K., Takashima, T., and Takayama, Y. 1988. Emissivity of pure and sea waters for the model sea surface in the infrared window regions. *Rem. Sens. Env.*, **24**, 313-329
- Segelstein, D.J. 1981. The complex refractive index of water. M.S. Thesis, University of Missouri, Kansas City, Missouri.
- Sherlock, V.J. 1999. ISEM-6: Infrared surface emissivity model for RTTOV-6. Forecasting Research Technical Report No.299, UK Met. Office, NWP division.

van Delst, P.F.W. and Wu, X. A high resolution infrared sea surface emissivity database for satellite applications. Technical Proceedings of The Eleventh International ATOVS Study Conference, Budapest, Hungary 20-26 September 2000, 407-411

Wu, X. and Smith W.L. 1997. Emissivity of rough sea surface for 8-13 μ m: modeling and verification. *Appl. Opt.*, **36**, 2609-2619.